Infrared Phys. Vol. 33, No. 5, pp. 345–357, 1992
Printed in Great Britain

0020-0891/92 $5.00 + 0.00
Pergamon Press Ltd

THE THEORY OF MULTIPLE QUANTUM-WELL GaAs–AlGaAs INFRARED DETECTORS

V. D. SHADRIN and F. L. SERZHENKO
Department of Theoretical Physics, Institute of Applied Physics, 111123, Moscow, U.S.S.R.

(Received 9 October 1991)

Abstract—The theory of multiple quantum-well GaAs–AlGaAs IR detectors based on the principle of quantum well photoionization is presented. The expression for the photoionization probability of the symmetric quantum-well is found to be exact in the effective mass approximation. Depolarization effects in the optical absorption spectra are discussed. We demonstrate that the depolarization shift of the spectrum maximum and its broadening lead to non-monotonic dependence of the photodetector detectivity on the electron concentration in wells in the background limited IR performance condition. The optimal factor of quantum-well filling, corresponding to the maximum of detectivity is rather small, and for the photoresistor with boundary wavelength $\lambda_1 = 10\,\mu$m, is $\theta = 0.10$.

We have also performed calculations for the concentration dependence of the transition temperature for background limited IR performance and found that for optimal concentrations it is about $T = 83$ K (for $\lambda_1 = 10\,\mu$m). The lifetime of non-equilibrium electrons is determined by capturing processes into the wells accompanied by emission of polar optical phonons and is $\tau \simeq 2 \times 10^{-11}$ s. The gain, along with the photoresistor sensitivity, is maximal for structures with a single quantum well.

I. INTRODUCTION

The present paper deals with the theory of multiple infrared (IR) GaAs–AlGaAs detectors based on the principle of photoionization of quantum well (QW). A detector operating on this principle and containing a single asymmetric QW was introduced[1] with the further elaboration of this concept.[2–4] Multiple GaAs–AlGaAs detectors with symmetric QWs operating on the optical ejection of electrons from the wells were first created by Levine *et al.*[5,6] and their parameters were comparable with those of the HgCdTe devices (operating on interband transitions). In contrast to detectors on intersubband transitions in QW,[7] detectors operating on the principle of well photoionization show smaller noise, as in the first instance it is necessary to apply a large electric field to receive high photoconductivity, which leads to the appearance of additional noise. QW detectors show an advantage over interband transition detectors in that high sensitivity occurs with negligible response times: however, the small lifetime of non-equilibrium electrons in the barrier region of the conduction band, determined by electron–phonon interaction, leads, as was noted,[8] to a lower temperature for the BLIP condition than in that of HgCdTe.

Various aspects of the IR QW detectors theory considered have been discussed in the above-mentioned papers.[1–4,8] Nevertheless, there is no general theory for photoelectric and threshold characteristics of detectors operating on the principle of QW photoionization.

The purpose of the present paper is to present this theory with calculations for properties of multiple GaAs–AlGaAs structures with symmetric QWs, which have been investigated.[5,6,9] The scheme of IR-radiation input also corresponds to the scheme used in these papers. Section II discusses the probability of photoionization of symmetric QW; Section III deals with the influence of concentration effects on the QW absorption spectrum; Section IV calculates the lifetime of electrons; Section V considers the theory of photoelectric characteristics: quantum efficiency, gain of photoresistor and sensitivity; Section VI calculates the BLIP transition temperature; and Section VII shows detectivity D_λ^* of a detector in the BLIP condition and performance optimization of a detector.

II. BOUND-TO-EXTENDED STATE OPTICAL ABSORPTION IN QUANTUM WELL HETEROSTRUCTURES

Let us consider the process of photoionization of a single symmetric QW where the QW is formed by two heterojunctions (Fig. 1). Within the framework of effective mass approximation for equal masses of electrons in both materials the problem is solved correctly. Under these conditions electrons behave as free in the direction of the plane that is perpendicular to the layers, i.e. dipole transitions are allowed only for radiation polarized perpendicular to the layers.

We normalize wave functions to the potential box with infinitely high walls under $x = +L$ (OX-axis is perpendicular to the layers). The potential is invariant under the X inversion, so all the wave functions are either even or odd. Optical transitions from the ground even state in the well are allowed only into the odd states of the continuous spectrum of the conduction band with the wave functions

$$|f> = S^{-1/2}\exp(i\mathbf{K}_{\parallel}\rho)\psi_{-}(x)$$

where, in compliance with[10] under $a \ll L$

$$\Psi_{-}(X) = \begin{cases} A_{-}\sin(Kx), & |x| \leqslant a. \\ \dfrac{\mathrm{sgn}(X)}{L^{1/2}}\sin(k(L-|x|), & |x| \geqslant a. \end{cases} \tag{1}$$

Here $\mathbf{k}_{\parallel}$ is an electron wave vector parallel to the plane of heterojunction, S is the surface area of the normalized volume $V = 2LS$, $K = (2m(U_0 + E_1)/\hbar^2 - k_{\parallel}^2)^{1/2}$, $k = ((2mE_1)/\hbar^2 - k_{\parallel}^2)^{1/2}$, m is the effective mass of the electron, $\hbar$ is Planck constant, U_0 is the depth of QW, $A_{-}^{-2} = L[1 + (K/k)^2\,\mathrm{ctg}^2(ka)]\,|\sin(ka)|$. E_1 is the energy, measured from the bottom of the conduction band of a wideband semiconductor.

The wave function of the ground state in the QW is

$$|i> = S^{-1/2}\exp(i\mathbf{k}\ \rho)\psi_0(X)$$

where

$$\Psi_0(x) = \begin{cases} A_0\cos(k_0 x), & |x| \leqslant a. \\ A_0\cos(k_0 a)\exp(-k_1(|x| - a)), & |x| \geqslant a. \end{cases} \tag{2}$$

Here $k_0 = (2m(U_0 - E_1))^{-1/2}/\hbar$, $k_1 = (2mE_1)^{-1/2}/\hbar$, $A_0 = (a + \lambda_0)^{-1}$, $\lambda_0 = k_1^{-1}$, and E_1 is the energy of the bottom of the 2-D subband.

The expression for the Hamiltonian interaction for photon absorption is

$$\hat{H} = -\frac{e}{mc}\left(\frac{2\pi N_v\hbar\omega}{Vq^2}\right)^{1/2}\exp(i(qx - \omega t))\hat{P}_x \tag{3}$$

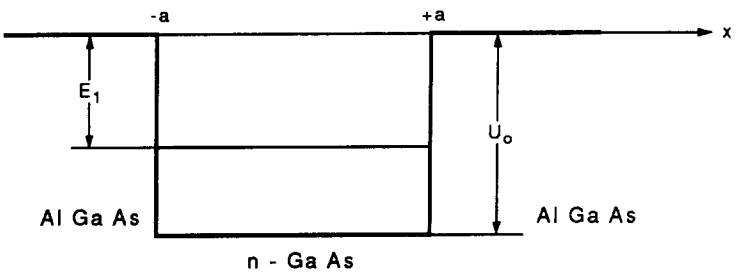

Fig. 1. Conduction-band diagram of a symmetric QW with ground state E_1 and depth U_0.

where N_v is the number of photons in volume V, $q = (\omega N_r c)$ is a photon wave vector, ω is a photon frequency, c is the light velocity, N_r is the refraction index, and $\hat{P}_x = -i\hbar(\partial/\partial x)$ is a projection of the momentum operator on the OX axis.

Using equations (1)–(3) we will get the radiation absorption rate, i.e. the transition frequency:

$$\tau^{-1} = \frac{(2\pi)^2 e^2 N_v}{V m^2 N_r^2 \omega} \sum (\langle f|\hat{P}_x|i\rangle)^2 f_0(E_i)(1 - f(E)\delta(E - E_i - \hbar\omega) \tag{4}$$

where $E_i = -E_1 + E_\perp$, $E_\perp = \hbar^2 k^2/(2m)$, $f_0(E) = (1 + \exp((E - E_{fe})/kT))^{-1}$ is a distribution function for electrons in the initial and $f(E)$ in the final states, E_{fe} is Fermi energy and T is temperature. Summation is taken with respect to the wave vectors $k_f = (k, \mathbf{k}_\parallel)$ of the final states of the electrons.

Momentum-matrix element $\langle f|\hat{P}_x|i\rangle$ calculated on the wave functions of localized (2) and delocalized (3) states is given by

$$\langle f|\hat{P}_x|i\rangle = \frac{2(1 - E_1)^{1/2}}{\omega(L(a + \lambda_0))^{1/2}} \left(1 + \frac{1 + E}{E} \operatorname{ctg}^2\left(\frac{a}{\lambda}(1 + E)^{1/2}\right)\right)^{-1/2} \tag{5}$$

In equation (5) all energies are normalized to the depth of the QW: $E_1 = (E_1/U_0)$, $E = (E_\perp/U_0)$, $\lambda = \hbar/(2mU_0)^{-1/2}$, $E_\perp = E - E$ is electron kinetic energy in a wideband semiconductor corresponding to its movement perpendicular to the plane of the heterojunction.

From equation (5) we note that the momentum-matrix element goes to zero under energies corresponding to the minima of amplitude A_- of the odd state (1) in a continuous spectrum over QW.

To proceed it is convenient to calculate the probability W of one-photon absorption which is related to the transition frequency τ^{-1} through the expression $W = (2LN_r/cN_v)\tau^{-1}$.

Changing from summing up to integrating over energies in equation (4) we obtain

$$W = \frac{(2^{1/2})e^2 L}{m^{1/2} N_r \omega \hbar^3 c} \int_0^\infty \frac{dE_\perp}{E_\perp^{1/2}} \int_0^\infty dE\ (\langle f|\hat{P}_x|i\rangle)^2 f_0(E_i)(1 - f(E))\delta(E_\perp + E_1 - \hbar\omega). \tag{6}$$

Integrating over E occurs over the electron energies in the 2-D subband due to conservation of parallel momentum. Integration over $E_\perp$ is facilitated by δ-functions, and for electrons in the ground state we receive

$$W = \frac{8e^2}{\hbar c} \frac{1}{N_r} \frac{\lambda}{a + \lambda_0} \frac{E_1(1 - E_1)\theta}{(\hbar\omega)^3(\hbar\omega - E_1)^{1/2}} F(\hbar\omega - E_1).$$

Here $\theta = (kT/E_1)\ln(1 + \exp(E_{fe}/kT))$ is the electron filling factor of the only QW-subband, and function $F(E)$ is given by

$$F(E) = \left(1 + \frac{1 + E}{E} \operatorname{ctg}^2\left(\frac{a}{\lambda}(1 + E)^{1/2}\right)\right)^{-1}.$$

It oscillates between zero and unity, while its maxima and minima correspond to the maximal and minimal values of amplitude A_-. Another characteristic feature of $W(E)$ is that it decreases considerably with an increase of the photon energy on the characteristic interval of U_0. Of special interest, therefore, is the spectrum of the transition probability near the boundary wavelength, i.e. for $E = (\hbar\omega E_1) \ll 1$. Noteworthy here is the phenomenon of resonance on the absorption threshold with $(a/\lambda) = (\pi/2)(2n - 1)$, $(n = 1, 2, 3, \ldots)$.

Under such relationships between the well parameters we get $W(E) \sim E^{-1/2}$. Under all the other meanings of the parameter (a/λ), except $(a/\lambda) = \pi n$, the absorption probability on the threshold can be expressed by $W(E) \sim E^{1/2}$. As for $(a/\lambda) = (\pi n)$ we get $W(E) \sim E^{5/2}$.

We can find the expression for the transition probability (6) under the conditions of the first $(n = 1)$ resonance. In this case there is one (even) subband in the well, and the next odd subband is virtual, i.e. it is "pushed out" into the state with energy $E_1 = 0$. The numerical calculation shows

that under $(a/\lambda) = (\pi/2)$ the lowest energy of the even subband $E_1 = 0.64$ lies below the continuum edge of the barrier. Taking into account $\lambda_0 = \lambda E_1^{-1/2}$ we have

$$W_{RES}(E) = 3.2 \times 10^{-3}\theta(E + 0.64)^{-3}E^{-1/2}.$$

Furthermore we get $W_{RES}(0.1) \simeq 0.7\%$ where $\theta = 0.3$ and $E = 0.1$. The average value over the interval $0 < E < 0.1$ is about 1.4%.

Figure 2 shows the spectrum $W(\lambda_{ph})$ as a function of photon wavelength for several values of the parameter $(a/\lambda) \leqslant (\pi/2)$ and for $\theta = 0.5$ when there is only one 2-D subband in QW with an electron Fermi level lower than the top of the QW.

We evaluate the absorption coefficient $\alpha_0(\omega) = (W/L)$ for a structure comprised of a series of QWs: where L is the period of the structure or the mean well-spacing, if the structure is non-periodic. Assuming that under resonance for the boundary wavelength $\lambda_1 = 10\,\mu$m, $a = 27$ Å and assuming $L = 250$ Å, we obtain, under resonance conditions, $\alpha_0 \simeq 1.5 \times 10^3\,\text{cm}^{-1}$ for $E = 0.1$, and an average value over the spectrum of $\langle a_0 \rangle = 3 \times 10^3\,\text{cm}^{-1}$. Using the relationship $\theta = (\pi\hbar^2 N_s)/(mE_1)$ where N_s is electron sheet concentration in QW, it is readily apparent that with $\theta = 0.3$ which corresponds to the threshold, $\lambda_1 = 10\,\mu$m can be obtained by doping the wideband part of the structure with $N_d = N_s/(L - 2a) \simeq 5 \cdot 10^{17}\,\text{cm}^{-3}$ or the narrowband part with $N_d = N_s/(2a) \simeq 2 \cdot 10^{18}\,\text{cm}^{-3}$.

Thus, under moderate doping a structure with a series of QWs possesses an absorption coefficient comparable with that of vertical interband transitions. Characteristic features of the photoionization spectrum are its oscillation as well as a prompt $(\hbar\omega)^{-3.5}$ decrease (as in the case of photoionization of a hydrogen-like impurity) when quantum energies considerably exceed ionization energy.

III. DEPOLARIZATION EFFECTS IN PHOTOIONIZATION SPECTRA OF QUANTUM WELLS

In Section II we discussed the coefficient of radiation absorption in structures with QWs in one-electron approximation. The results obtained prove that, from an absorption standpoint, "resonant" QWs are optimal, where the bottom of the second subband of quantum confinement

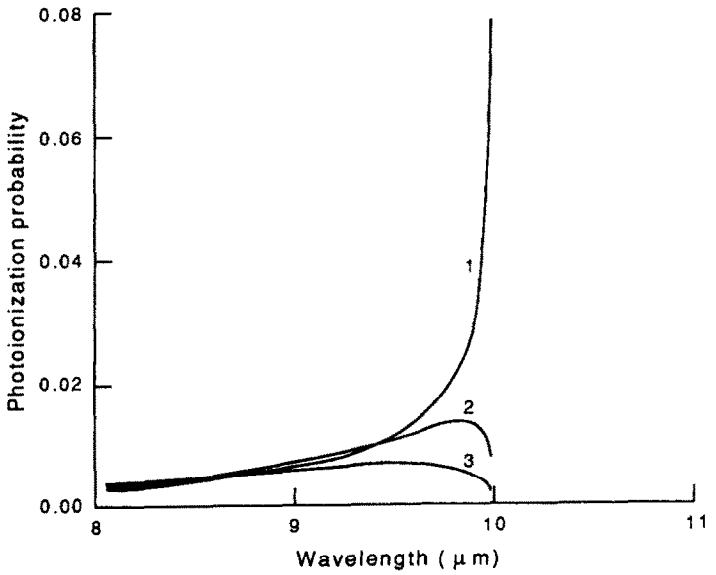

Fig. 2. The probability of photoionization of a single QW vs photon wavelength λ_{ph} for $\theta = 0.5$ and different values (a/λ): 1, $(a/\lambda) = (\pi/2)$; 2, $(a/\lambda) = 1.47$; 3, $(a/\lambda) = 1.37$.

coincides with the top of the well. Increasing electron concentration in wells increases the depolarization effects of incident radiation. These effects are especially pronounced for resonant wells near the absorption threshold because of the dramatic increase in the photoionization probability, and, consequently, the imaginary part of electron gas permittivity in QWs. Depolarization effects for the QW photoionization were considered for an asymmetric QW.[4]

Let us consider a rectangular resonant QW with half-width a and depth U_0. Let us assume that the permittivity of the layer containing electrons is $\epsilon_{xx} = \epsilon_1(\omega) + i\epsilon_2(\omega)$, and that of the non-absorbing layer is $\epsilon_{xx} = \epsilon_\infty$ where ϵ_∞ is high-frequency permittivity. We can express the value $\epsilon_2(\omega)$ through the probability of photoionization $W(\omega)$, calculated in Section II in a one-electron approximation $\epsilon_2(\omega) = (cN_r W(\omega))/(2\omega(a + \lambda_0))$, where λ_0 is the penetration depth of the electron wave function under the barrier.

In this paper we use Kramers–Kronig relation to find the real part of the permittivity layer.

$$\epsilon_1(\omega) = \epsilon_\infty + (2/\pi)\int_0^\infty (x\epsilon_2(x)/(x^2 - \omega^2))\,dx.$$

Figure 3 shows dependencies $\epsilon_1(\omega)$ and $\epsilon_2(\omega)$ near the absorption threshold for $\theta = 0.5$. It is readily apparent that $\epsilon_1(\omega)$ and $\epsilon_2(\omega)$ are comparable in magnitude near the absorption threshold of the region we are interested in. Dispersion $\epsilon_1(\omega)$ is also considerable. In view of the fact that $\epsilon_1(\omega)$ and $\epsilon_2(\omega)$ are comparable, in order to find the absorption coefficient of the electron-containing layer one should use the formula

$$\alpha_L(\omega) = (2\omega/c)Im(\epsilon_1 + i\epsilon_2)^{1/2}.$$

Even in the region of frequencies where $\epsilon_2(\omega) \ll \epsilon_1(\omega)$, and $\alpha_L(\omega) = (\omega/c)\,\epsilon_2(\omega)/(\epsilon_1(\omega))^{1/2}$, refractive index dispersion results in greater values of the layer absorption coefficient than those calculated in Section II, where this effect was neglected. If the structure with QWs has a period L, then the absorption coefficient calculated in terms of period of the structure is $\alpha_{ef}(\omega) = \alpha_L(\omega)(a_{ef}/L)$, where $a_{ef} = 2(a + \lambda_0)$ is the size of the localization of electron wave function in the first subband of quantum confinement.

We also extend our previous calculations to include those of the effective permittivity of the layer, with depolarization taken into account. The effective layer conductivity will be[11] normal to the layers $\sigma_{ef} = \sigma(\omega)\epsilon_\infty/(\epsilon_1 + i\epsilon_2)$, where $\sigma(\omega)$ is the layer conductivity without depolarization, ex-

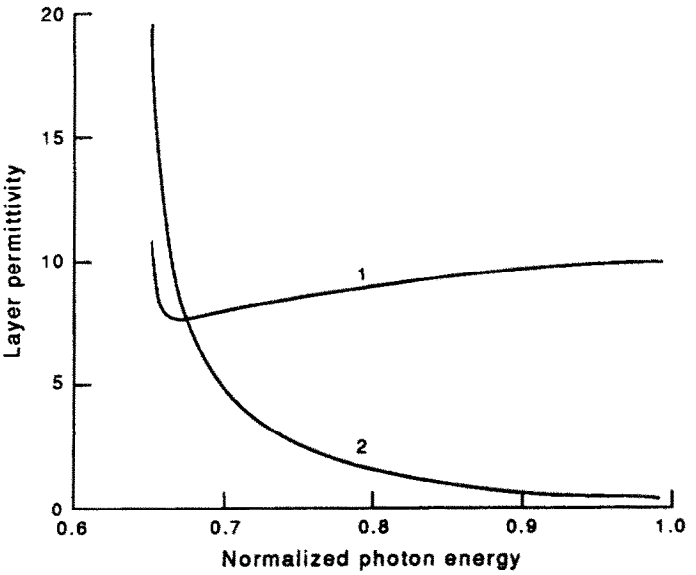

Fig. 3. Real and imaginary parts of the layer permittivity vs $(\hbar\omega/U_0)$, $\theta = 0.5$. 1, $\epsilon_1(\hbar\omega/U_0)$; 2, $\epsilon_2(\hbar\omega/U_0)$.

tracted from the equation $\epsilon_{xx}(\omega) = \epsilon_\infty + 4\pi i\sigma(\omega)/\omega$. The effective layer permittivity is then $\epsilon_{ef}(\omega) = \epsilon_\infty + 4\pi i\sigma_{ef}/\omega$.

Hence we get

$$Re\epsilon_{ef}(\omega) = \epsilon'_{ef}(\omega) = \epsilon_\infty(2 - \epsilon_1\epsilon_\infty/(\epsilon_1^2 + \epsilon_2^2))$$
$$Im\epsilon_{ef}(\omega) = \epsilon''_{ef}(\omega) = \epsilon_2\epsilon_\infty^2/(\epsilon_1^2 + \epsilon_2^2). \tag{7}$$

The absorption coefficient of the structure can be expressed by

$$\alpha_{ef}(\omega) = (2^{1/2}\omega/c)(a_{ef}/L)(((\epsilon''_{ef}(\omega))^2 + (\epsilon'_{ef}(\omega))^2)^{1/2} - \epsilon'_{ef}(\omega))^{1/2}. \tag{8}$$

The relationships (7) and (8) make it possible to obtain the absorption coefficient with depolarization taken into account. Figure 4 shows graphs of the functions $\alpha_{ef}(\omega)$ for the "resonant" structure GaAs–$Al_xGa_{1-x}As$ with the following parameters: $U_0 = 0.192$ eV, $m = 0.067m_0$, $\epsilon_\infty = 10.9$, $L = 250$ Å. Furthermore, $a = 27$ Å, $a_{ef} = 100$ Å and the photoionization threshold correspond to the wavelength $\lambda_1 = 10\,\mu$m, and the magnitude of the structure period has been selected from the condition of the weak overlap of the electron wave functions in neighbouring wells. Under the given concentration $\alpha_{ef}(\omega)$ is smaller than $\alpha_0(\omega)$ in the frequency region in the vicinity of the threshold, and exceeds $\alpha_0(\omega)$ outside this region. We emphasize that the result obtained here does not depend on the choice of the quantity L.

IV. ELECTRON LIFETIME IN A STRUCTURE WITH QUANTUM WELLS

In QW structures based on GaAs-AlGaAs polar semiconductors, the lifetime of non-equilibrium electrons is determined by their capture into wells accompanied by emission of polar optical phonons. Starting with the Hamiltonian expression for electron–phonon interaction

$$\hat{H}_{EF} = \sum_{\mathbf{q}} C(\mathbf{q}) \exp(i\mathbf{qr})(\hat{b}_{\mathbf{q}}^+ + \hat{b}_{-\mathbf{q}})$$

where $\mathbf{q}$ is the phonon wave vector and b^+, b are the phonon creation and annihilation operators, we obtain the following expression for capture rate (into a single well):

$$\tau^{-1} = \frac{2\pi}{\hbar} \sum_{\mathbf{q}} C^2(\mathbf{q}) |I(q_\perp)|^2 f_0(E_i)(1 - f(E))\delta(E - E_i - \hbar\omega). \tag{9}$$

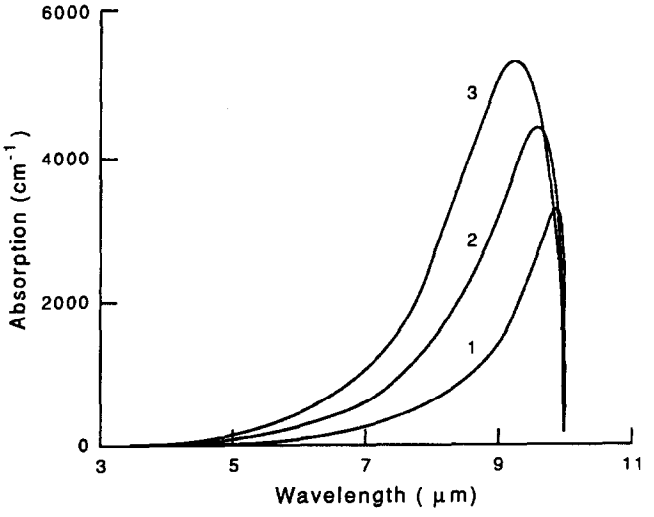

Fig. 4. Effective absorption coefficient vs wavelength of incident radiation for: 1, $\theta = 0.2$; 2, $\theta = 0.4$; 3, $\theta = 0.6$.

For electrons interacting with longitudinal polar optical phonons

$$C(\mathbf{q}) = C_0/(qV^{1/2}),$$

where $C_0^2 = 2\pi e^2\hbar\omega_i(\epsilon_\infty^{-1} - \epsilon_0^{-1})$ is the interaction constant,[12] $\hbar\omega_i$ is phonon energy, and ϵ_∞ and ϵ_0 are the high-frequency and static permittivity of the layers. We assume them to be the same for constituent semiconductors of the structure, so that we thereby neglect the phonon mode confinement; $f(E)$ is Fermi function, and $E_f = -E_1 + \hbar^2 k_\parallel^2/(2m)$ is the electron energy in the subband with a parabolic spectrum. The value of $I(q_\perp)$ in equation (9) is determined by the formula

$$I(q_\perp) = \int_{-L/2}^{L/2} \Psi_f^*(x)\exp(iq_\perp x)\Psi_i(x)\,dx$$

where $\Psi_i(x)$ and $\Psi_f^*(x)$ are the wave functions of the initial and the final electron states, which correspond to the movement perpendicular to the layers analogous to those presented in Section II, and L is the normalization length (period of the structure). In equation (9) the initial $\mathbf{p}_\parallel'$ and final $\mathbf{p}$ electron momenta in the plane of the layers are related by the conservation law $\mathbf{p}_\parallel = \mathbf{p}_\parallel' + \hbar\mathbf{q}_\parallel$, $\mathbf{q} = (q_\perp, \mathbf{q}_\parallel)$. Bearing in mind that at low temperatures $\mathbf{E}_i \simeq kT \ll \hbar\omega_i, E_1$ we obtain from equation (9)

$$\tau^{-1} = \frac{N_{ss}C_0^2}{\hbar}\int_{-\infty}^{\infty} \frac{I(q_\perp)f(E_f)}{\frac{2m}{\hbar^2}(E_1 - \hbar\omega_i) + q_\perp^2}\,dq_\perp$$

where $N_{ss} = m/(\pi\hbar^2)$ is the density of states in the subband.

To proceed we confine ourselves to the calculation of capture into a resonant QW, where the bottom of the second 2-D subband coincides with the top of the well. As is readily apparent from Sections II and III this is an optimal structure for achieving very high optical absorption. The value $I(q_\perp)$ in this case is given by the formula

$$|I(q_\perp)|^2 = \frac{4(1 - E_1/U_0)}{L(a + \lambda_0)}\,\frac{q_\perp^2}{\frac{2m}{\hbar^2}(E_1 - \hbar\omega_i) + q_\perp^2}.$$

As a result we have

$$\tau^{-1} = \frac{e^2}{\hbar L}\frac{\pi\lambda_0}{a + \lambda_0}\left(\frac{1}{\epsilon_\infty} - \frac{1}{\epsilon_0}\right)\frac{(\hbar\omega_i/E_1)(1 - E_1/U_0)}{(1 + (1 - \hbar\omega_i/E_1)^{1/2})^2} \times (1 + \exp((E_{fe} - E_1 + \hbar\omega_i - E_i)/kT)))^{-1}. \quad (10)$$

The last term of the formula takes into account occupancy of the final state in the subband, and decreases with Fermi level E_{fe} approaching the top of the well closer than the value $\hbar\omega_i$. For a GaAs–AlGaAs photodetector with wavelength $\lambda_1 = 10\,\mu$m ($E_1 = 0.124$ eV, $\hbar\omega_i = 0.036$ eV) the QW filling factor $\theta_0 = (1 - \hbar\omega_i/E_1)$, where the capture mechanism with optical phonon emission becomes inefficient, is equal to $\theta_0 \simeq 0.70$. However the optimal QW filling factor corresponding to maximum detectivity of background limited IR performance is considerably lower than θ_0, a fact apparent from further study.

Supposing the last term in equation (10) is equal to unity, for a GaAs–AlGaAs structure with $\lambda_1 = 10\,\mu$m, $\epsilon_\infty = 10.9$, $\epsilon_0 = 12.5$, $\hbar\omega_i = 0.036$ eV, and $L = 250$ Å, we obtain $\tau = 2 \times 10^{-11}$ s. The electron lifetime is proportional to the well-spacing.

V. PHOTOELECTRIC CHARACTERISTICS OF PHOTORESISTORS

Since we know the absorption coefficient $\alpha_{ef}(\lambda_{ph})$ and the electron lifetime τ in the conduction band we can calculate major photoelectric characteristics of the photodetector: quantum efficiency $\eta(\lambda_{ph})$, sensitivity S_i and gain G. It should be stressed here that, generally speaking, it is not possible

to calculate sensitivity and gain with manipulating magnitudes obtained in Sections II–IV. What we mean is that electrons participating in the conduction band over the wells get reflected. Remembering that there exists a possibility of the reflected electrons being captured into the well, the calculation of photocurrent in this case presents an independent problem. The present paper does not consider such a problem since it is apparent (as shown in Section II) that it is the resonant structure that would be optimal from the point of view of increasing $\alpha_{ef}(\lambda_{ph})$. The transmission coefficient for electrons over resonant wells is about unity for small energies, allowing one to treat the structure as the extrinsic photodetector, where emission of the electrons into the conduction band and their recombination are connected with the same wells.[13]

Another specifying circumstances to precede further calculations is the fact that the present paper deals with the photodetector on QWs, which assumes the presence of ohmic contacts in the structure. Contacts from n^+GaAs create barriers (at the expence of band bending), but the properly selected composition of n^+AlGaAs would be an ohmic contact.

In order to proceed with calculations it is useful to concretize the design of the photodetector with the help of the variant discussed[5] (Fig. 5). As was mentioned in Section II, QW photoionization is possible under the sole condition of radiation with polarization normal to the layers. We find the electric field magnitude in a light wave which has passed through prism into the bedded structure characterized by a mean refractive index $N_r = 3.5$ approaching the prism refractive index (for Si). The normal field component is $\epsilon_\perp = \epsilon_2 \sin \varphi_2$ where ϵ_2 is an absolute value of the electric vector in the plane of incidence in the medium 2. From Freunel equations we have

$$\epsilon_2 = 2\cos(\varphi)\sin(\varphi_2)/(\sin(\varphi + \varphi_2)\cos(\varphi - \varphi_2))\epsilon_1$$

where ϵ_1 is an absolute value of the electric vector in the plane of incidence in the medium 1.

The coefficient characterizing radiation introduced into the structure with normal polarization, with the application of an anti-reflection coating on the frontal surface of the prism is $K = (\epsilon_1/\epsilon_2)^2/2 \simeq (\sin^2\varphi)/2$ for unpolarized radiation, assuming $\varphi \simeq \varphi_2$. If the back surface of the photoresistor reflects radiation, quantum efficiency of the QW photodetector is given by

$$\eta(\lambda_{ph}) = (1 - \exp(-2\alpha_{ef}(\lambda_{ph})l))\sin^2(\varphi)/2.$$

Figure 6 shows numerically calculated quantum efficiencies of the QW photodetector with a boundary wavelength $\lambda_1 = 10\,\mu$m. These formulae and relationships are obtained from depolarization effects (Section III) for three impurity concentrations $N_s = \theta N_0$, where $N_0 = (mE_1)/(\pi\hbar^2)$ is

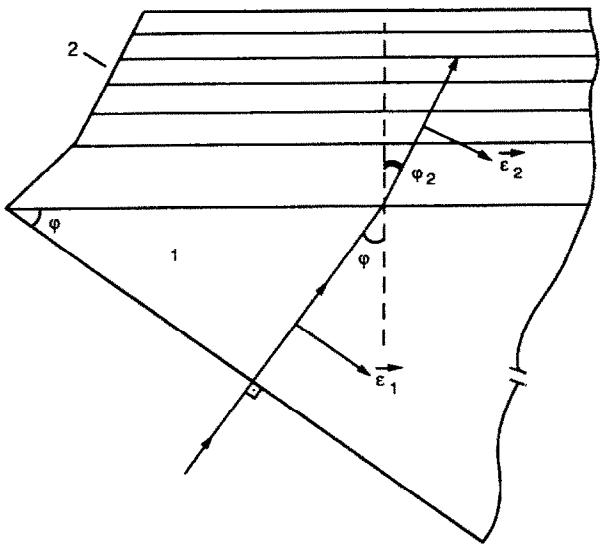

Fig. 5. Scheme of radiation input. 1, Si-prism; 2, QW-structure.

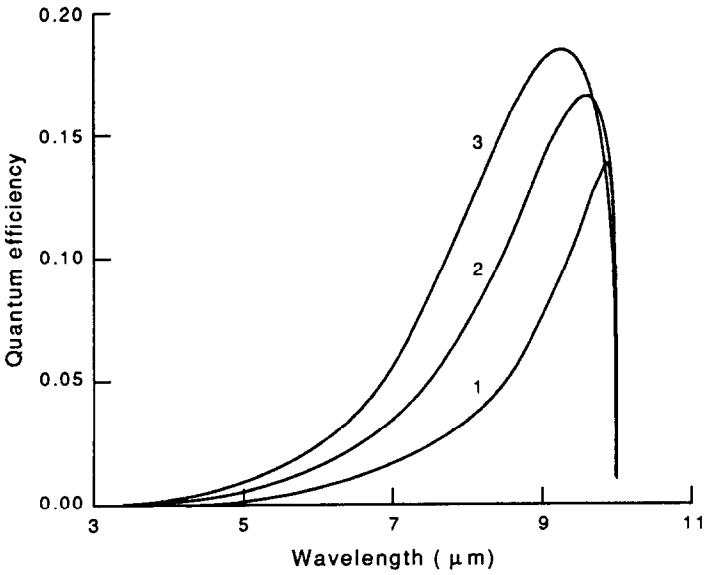

Fig. 6. Quantum efficiency of a multiple QW GaAs–AlGaAs photodetector: $L = 250$ Å, $N = 50$, $\varphi = 45^{\circ}$, $\lambda_1 = 10\mu$m. 1, $\theta = 0.2$; 2, $\theta = 0.4$; 3, $\theta = 0.6$.

the electron sheet concentration indicative of complete filling of the well. The respective 3-D concentration of impurity as regards the well width is $N_d = N_s/(2a)$, and with $\lambda_1 = 10\,\mu$m is $N_d = \theta \cdot 6.4 \cdot 10^{18}\,\text{cm}^{-3}$ when $a = 27$ Å.

As can be understood from Fig. 6 the curves $\eta(\lambda_{ph})$ register the form analogous to $\alpha_{ef}(\lambda_{ph})$, which is not surprising since the inequality $2\alpha_{ef}l > 1$ is achieved for a maximum α_{ef} only for $N = (l/L) = 50$. In the remaining region $2\alpha_{ef}l < 1$ and we have approximately $\eta(\lambda_{ph}) = \alpha_{ef}(\lambda_{ph})l$.

The width of the curve $\eta(\lambda_{ph})$ depends on the electron concentration in the well. Our further investigations (Section VII) show that the depolarization shift of the maximum η_{max} into a short wavelength region and broadening $\eta(\lambda_{ph})$ which occurs with an increase in concentration, lead to lower detectivity of the photodetector in the region of large electron concentrations.

Another important characteristic is sensitivity: $S_i = (I_f/P_f)$ where I_f is the photocurrent, $P_f = hvI_0$ is the power of the received radiation, v is the frequency of the photons, and I_0 is the photon flux. The photocurrent in the short circuit mode is given by

$$I_f = \int_0^l (eS/l)\,\Delta n v_\perp \,dx$$

where S is the surface area of the photodetector, $v_\perp$ is the drift velocity of photogenerated carriers, $\Delta n = g_T\tau$, g_T is the rate of carrier generation: $g_T = \alpha_{ef}I(x)$, where $I(x)$ is the photon flux through the cross-section of the photodetector with coordinate x. In the scheme with a reflective back surface $I(x) = I_0\,\text{ch}(\alpha_{ef}(x - l))$. Thus we have $S_i = (e/\hbar\omega)\eta G$, where $G = \tau v_\perp/l$ is the photoresistor gain, and $W = L/(\tau \cdot v_\perp)$ is the probability of an electron capture into the ground state of the QW. We can express the formula for S_i in the following form: $S_i = (S_i)_{max} f(2\alpha_{ef}l)$ where $f(x) = (1 - \exp(-x))/x$ is the function with a maximum under $f(0) = 1$. $(S_i)_{max} \simeq (e/\hbar\omega)(\alpha_{ef}L/W)$ is a maximum of sensitivity.

As is apparent from the last formula, the photoresistor sensitivity is maximal for a single QW, with the rather small quantum efficiency being compensated for by the maximal gain for such a resistor, $G = (1/W) \propto v_\perp$.

With the number of wells increasing, the growth η_{max} occurs more slowly than the decrease of the gain $G = (1/NW)$. This unusual dependence of sensitivity on the number of wells is connected with the fact that photogeneration and non-equilibrium electron capturing are related to the same

wells. However, remembering that with lower concentrations $N_s < (N_0/2)$ the magnitude $\alpha_{ef}L$ represents $(\alpha_{ef}L) \leqslant 10^{-2}$ it should be noted that a decrease of S_i is negligible even for $N = 50$, so even on the frequencies corresponding to maximum quantum efficiency $S_i \simeq (S_i)_{max}$.

In summary we present evaluations for the gain. In the field $E \leqslant 10^4$ (V/cm) the electron drift velocity reaches $v_\perp = 10^7$ (cm/s). Then, drawing on the estimation $\tau \simeq 2 \times 10^{-11}$ s obtained in Section IV for a structure with $L = 250$ Å, $\varphi = 45°$ we have $G_{max} = (\tau v_\perp)/L \simeq 80$.

For sensitivity we obtain the estimation drawing on $(\alpha_{ef})_{max}L \simeq 5 \times 10^{-3}$:

(a) $\lambda_1 = 10\,\mu$m; $(S_i)_{max} \simeq 0.6$ A/W.
(b) $\lambda_1 = 12\,\mu$m; $(S_i)_{max} \simeq 0.8$ A/W.

VI. THE TEMPERATURE OF BLIP CONDITION

Under low temperatures generation–recombination noise dominates in the photoresistor, evoked by the thermal or background generation processes. The most favorable for maximum detectivity is the mode where the generation–recombination noise initiated by the background predominates. The temperature of the transition into the mode where background radiation-initiated noises predominate, can be obtained from the equation $g_T = g_B$, where

$$g_T = \int_{\nu_1}^{\infty} \eta(\nu)\Phi_B(\nu)\,d\nu/l$$

is the rate of electron generation in the course of background radiation absorption. $\Phi_B(\nu)$ is the spectral density of the photon background flux. For blackbody radiation with temperature T_B we have:

$$\Phi_B(\nu) = (2\pi\nu^2/c^2)[\exp(h\nu/kT_B) - 1]^{-1}.$$

We can now determine the rate of carrier generation g_T. As was mentioned earlier in Section V, the photoresistor under generation–recombination equilibrium is considered, then $g_T = (n_T/\tau)$ where n_T is the dark concentration of carriers in the conducting states.

Let us return to the correlation determining the temperature for BLIP. In order to determine that temperature we obtain:

$$\frac{\tau}{L}\int_{\nu_1}^{\infty} \frac{(1 - \exp(-2\alpha(\nu)\cdot l))}{2N}\Phi_B(\nu)\,d\nu\,\sin^2\varphi = N_c(T)\exp(-E_1/kT)[\exp(\theta E_1/kT) - 1]. \quad (11)$$

Equation (11) was numerically calculated based on the values of the absorption coefficients from Section III. The transition temperatures into BLIP are plotted on the graphs for photoresistors with boundary wavelengths $\lambda_1 = 10\,\mu$m and $\lambda_1 = 12\mu$m (Fig. 7). As can be readily seen the maximal transition temperature for $\lambda_1 = 12\,\mu$m reaches a temperature close to that of liquid nitrogen.

For $\lambda_1 = 12\,\mu$m we have $T_{max} \simeq 72$ K for $\theta = 0.10$ or $N_d \cong 4.7 \cdot 10^{17}$ cm^{-3}. Under such concentrations the photoresistor possesses a small quantum efficiency (Fig. 4). An increase of θ results in a decrease of temperature. We note the weak dependence of T on the number of wells N connected with the weak dependence of $f(x) = (1 - \exp(-x))/x$ on N under $x = 2\alpha(\omega)\cdot l < 1$.

Our calculations lead to the results cited in the present section, $T \simeq 83$ K for a photoresistor with a boundary wavelength $\lambda_1 = 10\,\mu$m which exceeds the temperature estimated in Ref. (8). Low BLIP temperatures in comparison with HgCdTe photodetectors are conditioned by two reasons. The first one is small lifetime $\tau \simeq 2 \times 10^{-11}$ s of carriers in the conduction band as opposed to HgCdTe with $\tau \simeq (10^{-7} - 10^{-6})$ s. The second reason is connected with the lower threshold of electron thermal generation into the conduction band in comparison with the photoelectric threshold, as magnitude $E_{fe} = (\pi\hbar^2/m)N_s$ grows with an increase of N_s and, consequently θ.

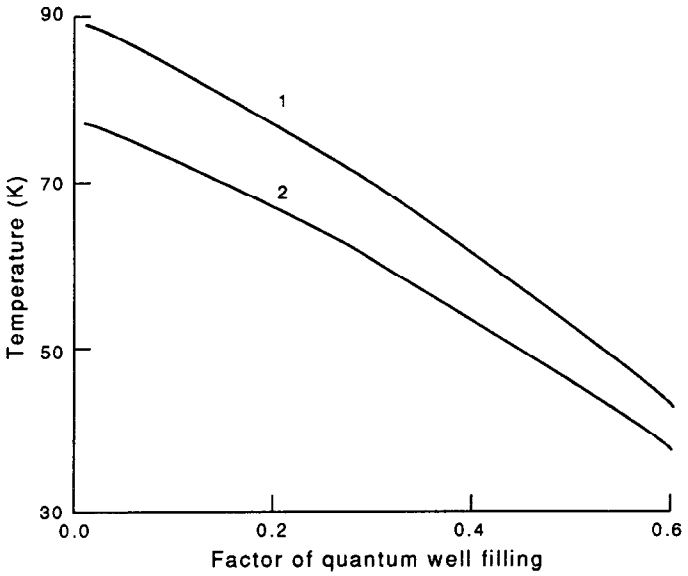

Fig. 7. The temperature of BLIP vs electron filling factor θ. 1, $\lambda_1 = 10\,\mu$m; 2, $\lambda_1 = 12\,\mu$m.

The following section will show, nevertheless, that an optimal condition exists for BLIP with a rather small concentrations N_s, where the most important characteristic of a photodetector detectivity $D^*_\lambda(\theta)$ has a maximum.

VII. DETECTIVITY OF A QUANTUM WELL PHOTORESISTOR

The detectivity of a photoresistor for monochromatic radiation with a wavelength $\lambda_s = (c/\nu_s)$ when background limited IR performance is achieved, equals[14]

$$D^*_\lambda = \frac{\eta_s}{2h\nu_s}\left[\int_{\nu_1}^{\infty} \frac{\exp(h\nu/kT_B)}{\exp(h\nu/kT_B)-1}\,\Phi_B(\nu)\eta(\nu)\,d\nu\right]^{-1/2} \tag{12}$$

In equation (12) radiation is received into a semisphere, where η_s is the quantum efficiency of a photodetector on the frequency ν_s of a signal radiation.

Assuming that BLIP is achieved we can now determine D^*_λ for the QW (GaAs–AlGaAs) photoresistor. In order to perform the calculations we use quantum efficiency of the QW photodetector from Section V, with the effect of depolarization of the received radiation (Section III) being taken into account.

Figure 8 shows the dependencies of $D^*_\lambda(\theta)$ for $\lambda_1 = 10\,\mu$m and $\lambda_1 = 12\,\mu$m. The frequency of a signal radiation for every concentration corresponds to the function maximum $\eta(\nu)$ where $\nu = c/\lambda_{ph}$ (see Fig. 4).

As can be seen from Fig. 8, the depencence $D^*_\lambda(\theta)$ registers the maximum, which corresponds to $N_d = N_a/(2a) \simeq 6.4 \cdot 10^{17}\,\text{cm}^{-3}$ for $\lambda = 10\,\mu$m i.e. rather small concentration values.

So, in contrast to widespread opinion an increase of $\eta(\nu_s)$ accompanying the growth of θ does not mean that $D^*_\lambda(\theta)$ increases. Such a correlation occurs at the initial stage of the dependence $D^*_\lambda(\theta)$. Further stages show a decrease of D^*_λ though $\eta_s(\theta)$ increases. It happens because the spectrum width $\eta(\nu)$ influences the magnitude of the background flux received. Under small θ the curve $\eta(\nu)$ is narrow, and its maximum corresponds to $\eta(\nu_s) \ll 1$. An increase of $D^*_\lambda(\theta)$ is accompanied by both θ and curve width $\eta(\nu)$.

The growth of the received background radiation occurs as a result of the increase in radiation bandwidth received, rather than an increase in the maximum $\eta(\nu_s)$. As a result $D^*_\lambda(\theta)$ decreases with the increase of θ for concentrations greater than some finite figure. The initial stage growth

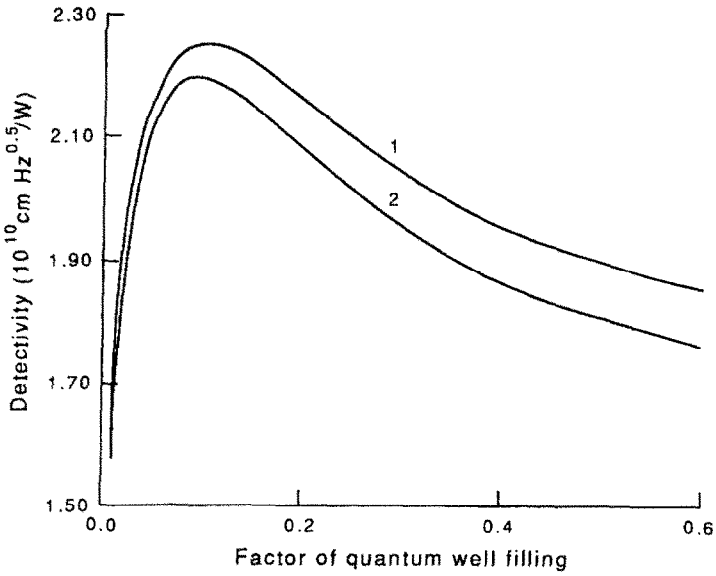

Fig. 8. Detectivity of a QW photoresistor in BLIP vs electron filling factor θ; $L = 250$ Å, $N = 50$, $\varphi = 45°$. 1, $\lambda_1 = 10\,\mu$m; 2, $\lambda_1 = 12\,\mu$m.

of $D_\lambda^*(\theta)$ evokes growth of θ, at the expense of the growth of maximum $\eta(\nu_s)$. Thus the depolarization effects influence on the width and magnitude of $\eta(\nu_s)$ is actually felt in the dependence of the threshold characteristics on the doping impurity concentration, resulting in a lowering of detectivity in the large electron concentrations in the subband. The curves in Fig. 8 can be considered as optimization of $D_\lambda^*(\theta)$ by the parameter θ. The unusual dependence $D_\lambda^*(\theta)$ prompts the conclusion that the BLIP temperature of the optimized GaAs–AlGaAs structure for $\lambda_1 = 10\,\mu$m, and for $\Omega = 2\pi$ is taken to be $T \simeq 83$ K.

In summary, we note that the influence of depolarization effects on the spectrum $\alpha_{ef}(\lambda_{ph})$, and $\eta(\lambda_{ph})$ on the concentration dependence of the threshold characteristics of a QW photodetector, discussed above (Section III), leads to rather small magnitudes of the optimal concentrations of the doping impurity corresponding to the maximal possible for the given structure BLIP temperatures. The result obtained allows a more optimistic evaluation in comparison with the prospects of QW photodetector application as an alternative to HgCdTe photodetectors.

VIII. CONCLUSION

Summing up the theory of photoelectric and threshold characteristics of QW (GaAs–$Al_xGa_{1-x}As$) photodetectors introduced in the present paper, we want to emphasize the major specific features of these structures when applied as radiation receivers.

(1) The absorption coefficient for IR radiation in the process of QW photoionization can be of the same order as the absorption coefficient in direct interband transitions provided a fairly high concentration of the doping impurity is maintained.
(2) Depolarization effects are significant in the process of absorption radiation $\lambda = 8$–$12\,\mu$m for the doping concentration $N_d > 10^{17}$ cm^{-3}. Depolarization shift and the change of the absorption spectrum determine the magnitude of the absorption coefficient and the received frequency bandwidth.
(3) The optimal condition as regards maximum absorption is a resonant structure with QWs containing the virtual second subband of quantum confinement.
(4) The QW photodetector is characterized by a narrow bandwidth with $(\Delta\lambda/\lambda) \simeq 0.1$. The maximal magnitude of the quantum efficiency does not exceed 50%.

(5) The non-equilibrium electron lifetime is determined by the process of their being captured into wells under emission of polar optical phonons. The lifetime does not depend on the applied electric field (for low fields) and is $\tau = 2 \times 10^{-11}$ s for GaAs–AlGaAs structure.
(6) The gain of the QW photoresistor is proportional to the drift velocity, maximal for the structure containing the only QW and is $G \simeq 80$.
(7) Maximum of sensitivity is also achieved on the structure with the only QW or small number of them, where $2\alpha_{ef}L \ll 1$ and is taken to be $(S_i)_{max} \simeq (e/\hbar\omega)\,(\alpha_{ef}LG_{max})$. For the optimal photoresistor with $\lambda_1 = 10\,\mu$m the estimation gives $(S_i)_{max} \simeq 0.6\,(A/W)$.
(8) The effects of depolarization shift and photoabsorption spectrum broadening determine unconventional dependence of BLIP detectivity on the doping impurity concentration. This is accompanied by the increase of D^*_λ for small concentrations, evoked by an increase of quantum efficiency maximum η, and for small concentrations it decreases with spectrum broadening of $\eta(\lambda_{ph})$.
(9) Optimal concentration corresponding to the maximum D^*_λ for BLIP is $N_d \simeq 6.4 \cdot 10^{17}\,\text{cm}^{-3}$ ($\lambda_1 = 10\,\mu$m). Here the quantity D^*_λ for the flux $\Phi_B = 5 \times 10^{17}\,\text{cm}^{-2}\,\text{s}^{-1}$ depends on the number of wells and for $N = 50$ is given by $D^*_\lambda(\lambda_1 = 10\,\mu\text{m}) = 2.25 \times 10^{10}$ (cm $\text{Hz}^{0.5}$/W).
(10) The optimum for D^*_λ concentrations corresponds to concentrations where the maximum photodetector BLIP temperature T is achieved. For a photodetector with $\lambda_1 = 10\,\mu$m (background radiation flux $\Phi_B = 5 \times 10^{17}\,\text{cm}^{-2}\,\text{s}^{-1}$) $T = 83$ K.

REFERENCES

1. D. D. Coon and R. P. G. Karunasiri, *Appl. Phys. Lett.* **45,** 469 (1984).
2. D. D. Coon, R. P. G. Karunasiri and H. C. Lill, *J. appl. Phys.* **60,** 2636 (1986).
3. K. W. Goossen and S. A. Lyon, *Appl. Phys. Lett.* **47,** 1257 (1985).
4. K. W. Goossen and S. A. Lyon, *J. appl. Phys.* **63,** 5149 (1988).
5. B. F. Levine, C. G. Bethea, G. Hasnain, J. Walker and R. J. Malik, *Electronics Lett.* **24,** 747 (1988).
6. B. F. Levine, C. G. Bethea, G. Hasnain, J. Walker and R. J. Malik, *Appl. Phys. Lett.* **53,** 296 (1988).
7. K. K. Choi, B. F. Levine, C. G. Bethea, J. Walker and R. J. Malik, *Appl. Phys. Lett.* **50,** 1814 (1987).
8. M. A. Kinch and A. Yariv, *Appl. Phys. Lett.* **50,** 2093 (1989).
9. B. K. Janousek, M. J. Daugherty, W. L. Bloss, M. L. Rosenbluth, M. J. O'Loughlin, H. Kanter, F. J. De Luccia and L. E. Perry, *J. appl. Phys.* **67,** 7608 (1990).
10. S. Flugge, *Practical Quantum Mechanics*, Vol. I. Springer-Verlag, Berlin. (1971).
11. T. Ando, A. Fowler and F. Stern, Electronic properties of two dimensional systems. *Rev. Mod. Phys.* **54,** No. 2 (1982).
12. E. M. Conwell, *High Field Transport in Semiconductors*. Academic Press, New York (1967).
13. F. L. Serzhenko and V. D. Shadrin, *Sov. Tech. Phys. Lett.* **35,** 171 (1990).
14. R. J. Keyes, *Optical and Infrared Detectors*, Springer-Verlag, Berlin (1980).